

Wurster's crownophanes: an alternate topology for *para*-phenylenediamine-based macrocycles

John W. Sibert,^{a,*} Greg R. Hundt,^a Andrew L. Sargent^{b,*} and Vincent Lynch^c

^aDepartment of Chemistry, The University of Texas at Dallas, PO Box 830688, Richardson, TX 75083-0688, USA

^bDepartment of Chemistry, East Carolina University, Greenville, NC 27858, USA

^cDepartment of Chemistry, The University of Texas at Austin, Austin, TX 78712, USA

Received 15 July 2005; revised 20 September 2005; accepted 21 September 2005

Available online 14 October 2005

Abstract—Six redox-active cyclophane/crown hybrid molecules (crownophanes) were prepared via cyclization reactions involving *N,N'*-dimethyl-*p*-phenylenediamine and tosylated oligoethylene glycols of varying length. These new host molecules differ from other phenylenediamine-containing crown ethers in that the electron-rich π face is designed to be part of the ligating group. Their electrochemical properties were determined by cyclic voltammetry with a correlation found between macrocyclic architecture and ease of oxidation. The affinity of the smaller crownophanes for cations was studied by cyclic voltammetry with the result that these hosts show no electrochemical response to alkali metal cations, but, dependent on macrocycle size, modest selectivity for alkaline earth metal cations. This stands in contrast to previously reported phenylenediamine-containing crown ethers in which the redox centers are linked to guest ions through a macrocyclic amino group.

© 2005 Elsevier Ltd. All rights reserved.

1. Introduction

Macrocycles containing electrochemically active subunits are of interest because of their ability both to sense bound guest species and control the coordination environment of the host.¹ We² and others³ have previously prepared a series of redox-active ligands centered around the electrochemically active phenylenediamine structure. The ligands reported to date have been referred to as 'Wurster's crowns' (see Fig. 1) because they are formally derived from the famed Wurster's reagent (*N,N,N',N'*-tetramethyl-*p*-phenylenediamine or TMPD).⁴ In all reported examples, the phenylenediamine moiety has been attached to a crown ether by a single phenylenediamine nitrogen atom within

the macrocycle framework. Such structures preserve the rich electrochemical properties of the phenylenediamine subunit, thereby allowing for the sensing of bound metal ions via the accompanying change in ligand oxidation potential upon coordination.

Motivated by the efficient metal binding properties of the Wurster's crowns, we became interested in an alternate structural motif for incorporating the electrochemically active phenylenediamine unit into the body of a crown. In these macrocycles, both N atoms of the phenylenediamine moiety are now contained within the macrocyclic framework to produce hybrid crown/cyclophane⁵ structures called 'Wurster's crownophanes' (see Fig. 1). Similar to previously

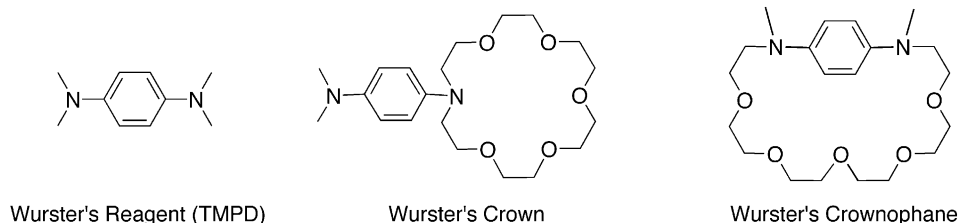


Figure 1. Representative macrocycles derived from Wurster's reagent (*N,N,N',N'*-tetramethyl-*p*-phenylenediamine or TMPD).

Keywords: Cyclophane; Crown; Crownophane; Wurster; Redox.

* Corresponding author. Tel.: +1 972 883 2918; fax: +1 972 883 2925.; e-mail: sibertj@utdallas.edu

reported redox-active crown ethers, these hosts are designed to be electrochemically responsive to cations. However, the mode of communication between the redox center and guest ions in presumed endocyclic complexes should prove quite distinct, occurring through the electron-rich π face of the phenylenediamine moiety and not the amino group. In addition to potential utility in electrochemical sensing and/or switching applications, these compounds may prove useful in probing hard cation- π interactions, a topic of considerable recent interest due to an established significance in controlling protein folding and enzyme-substrate recognition.⁶

Related crownphanes containing the electron-rich π systems 1,4-dialkoxybenzene⁷ and tetrathiafulvalene (TTF)⁸ have been previously reported. In the latter case, the reversible electrochemistry of TTF has led to their study as electrochemical sensors for metal cations. It is worth noting that these ligands are typically synthesized as mixtures of *Z* and *E* isomers. Further investigation by mass spectrometry has indicated that the *Z* isomer alone participates in binding allowing for the TTF moiety to potentially interact either through the π system, heterocyclic S atoms or through distortions of the π system caused by complex formation.

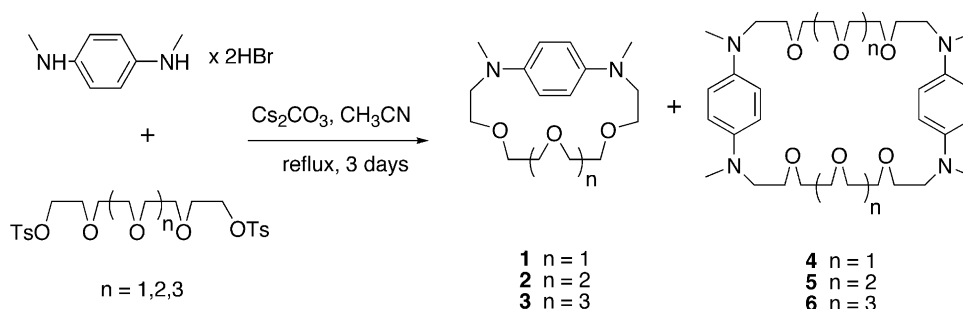
Both Staab, et al.⁹ and, more recently, Takemura, et al.¹⁰ have reported on the redox properties and charge transfer complexes of Wurster-type cyclophanes containing phenylenediamine subunits. In both studies, the cyclophanes contain alkyl linkages between two *p*-phenylenediamine subunits and were, therefore, not designed nor studied for metal chelation. Interestingly, however, the length of the alkyl spacers and their respective points of attachment on the phenylenediamine subunits gave clear differences in the resulting electrochemical properties of the cyclophanes with shorter linkages giving rise to cooperative effects between the two redox centers.

In this report, we describe the synthesis and properties of Wurster's crownphanes along with unanticipated larger macrocyclic byproducts and explore their ability to complex hard cations.

2. Results and discussion

2.1. Ligand synthesis

As shown in Scheme 1, the synthesis of macrocycles **1**, **2**



Scheme 1.

and **3** was accomplished using a general method that can be extended by choice of electrophile to produce a range of redox-active crownphanes. Specifically, *N,N'*-dimethyl-*p*-phenylenediamine dihydrobromide, an oligoethylene glycol ditosylate of appropriate length (tetraethylene glycol for **1**, pentaethylene glycol for **2**, hexaethylene glycol for **3**), and carbonate base were refluxed for 3 days in acetonitrile to yield the desired ligands. Following radial chromatography on alumina, the crownphanes were isolated in approximately 20–25% yield as light brown oils. Shorter reaction times revealed the presence of significant amounts of starting materials as monitored by thin layer chromatography (TLC) while longer reaction times gave no improvement in cyclization yields. Further, the reaction yields were largely insensitive to the choice of alkali metal carbonate used as base. While the yields are modest, the products can be quickly and definitively identified by TLC analysis. *N*-peralkylated *p*-phenylenediamines, like TMPD, oxidize upon exposure to UV light resulting in the characteristic blue color of the radical cation. As such, TLC analysis of successful crude reaction mixtures show the presence of a 'Wurster's blue' spot that can be attributed to the formation of the target Wurster's crownophane. However, during the preparation of the anticipated products **1**, **2** and **3**, additional products were formed as evidenced by the presence of a second 'Wurster's blue' spot on the TLC of each crude reaction mixture. These minor products proved to be the larger '2+2' cyclization crownphanes **4**, **5**, and **6**, isolated from the reaction mixtures in approximately 3–5% yield. These larger macrocycles are currently being studied for their utility in the assembly of more intricate supramolecular structures (e.g., rotaxanes and catenanes).

2.2. Crystallographic study of **4**

Unlike the smaller crowns **1**, **2** and **3**, which were isolated as thick oils, macrocycle **4** is a crystalline solid. In fact, the crude reaction mixtures containing **1** and **4** can be separated by recrystallization from methanol with **4** forming crystals and **1** remaining in solution. As shown in Figure 2, **4** contains a large cavity with dimensions of 6.4 Å (from the centroid of one aromatic ring to the other) by 14.4 Å. The two methyl groups are positioned 'trans' with respect to the phenyl moiety. Individual molecules of **4** are stacked in the crystal lattice to give long channels throughout the structure (Fig. 3). The closest π - π distance between neighboring molecules (6.6 Å) rules out the possibility of intermolecular π - π stacking.

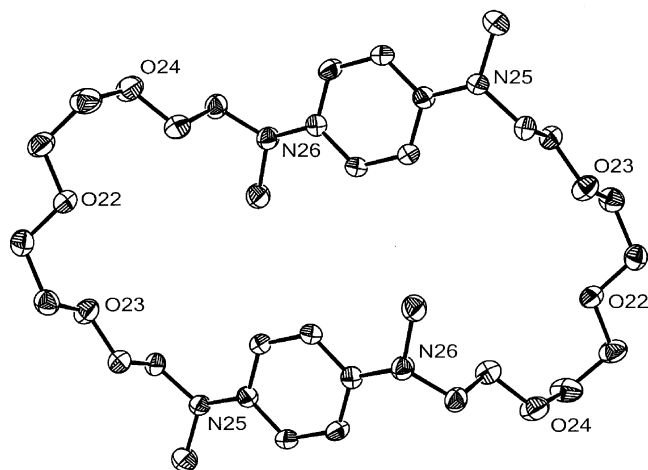


Figure 2. X-ray crystal structure of **4** showing the atom labeling scheme. Displacement ellipsoids are scaled to the 50% probability level with H atoms omitted for clarity.

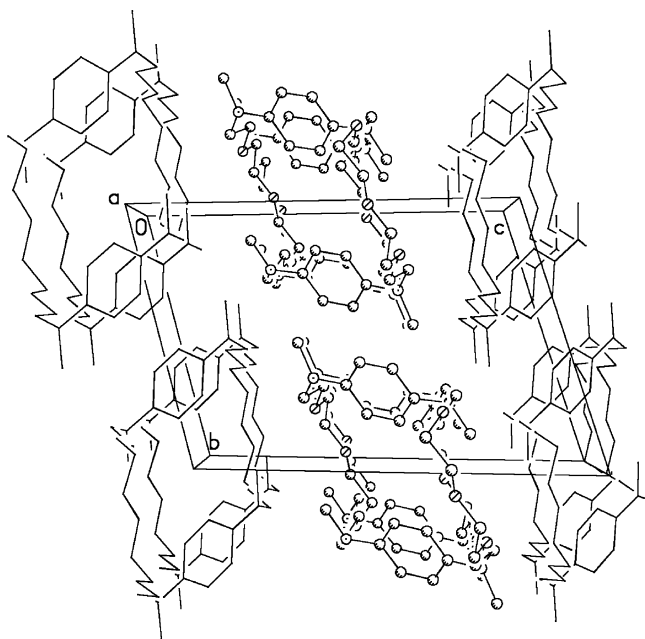


Figure 3. Unit cell packing diagram for **4**. The view is approximately down the *a*-axis. Crystallographic structures **1** are shown in ball-and-stick fashion while crystallographic structures **2** are in wireframe display form.

2.3. Electrochemistry

Cyclic voltammetry was used to explore the relationship between the electrochemical properties of **1–6** and ligand architecture. All six compounds show two reversible one-electron oxidations, like TMPD. For the larger cyclophanes **4–6**, the two phenylenediamine subunits behave as independent redox centers as might be expected considering the long aliphatic linkages between them. In fact, Takemura, et al. demonstrated that a five carbon chain between two *p*-phenylenediamine units is sufficient for the redox centers to behave as discrete electrochemical entities.¹⁰ As shown in Table 1, the smaller Wurster's crownphanes oxidize more easily than TMPD with the effect strongest for the smallest crownophane **1**. Considering the three larger cyclophanes **4**, **5** and **6** oxidize at

Table 1. Half-wave potentials (vs Ag/AgCl, 0.1 M TEABF₄, CH₃CN, 100 mV/s) of TMPD and Wurster's crownphanes **1–6**

Compound	$E_{1/2}$ (mV)	$E_{1/2}$ (mV)
TMPD	124	708
1	64	677
2	70	697
3	93	709
4	132	743
5	131	753
6	128	734

potentials similar to that of TMPD, the facile oxidation of **1**, **2** and **3** must be associated with their common intramolecular arrangement of a polyether fragment directly across from the redox center. That **1** exhibits the most facile oxidation (60 mV easier to oxidize than TMPD) indicates that its smaller ring size positions the polyether subunit closest to the phenyl ring and, thus, best able to stabilize the radical cation formed upon oxidation. An alternate explanation is that compound **1** has the most electronic strain between the dipoles created by the ether groups and the electron rich π system. This strain is relieved by oxidation which allows for a favorable electrostatic interaction between the polyether and radical cationic phenylenediamine subunits (vide infra).

Cyclic voltammetry was also used to probe the electrochemical responses of **1**, **2**, and **3** to various hard cations. Indeed, both aniline¹¹ and phenylenediamine-containing crown ethers^{2a,2b,3c} respond to the coordination of cations through anodic shifts in their oxidation potentials. For the alkali metal cations, the magnitude of the response correlates well to complex stabilities. The electrochemical responses of the Wurster's crownphanes (as measured by a shift in the first oxidation potential of the phenylenediamine unit) after addition of 1.2 equiv of metal or ammonium salts were analyzed. Interestingly, and in contrast to redox-active crown ethers, the Wurster's crownphanes show no evidence for the binding of alkali metal ions. However the first oxidation potential of the largest crownophane, **3**, shifts anodically in the presence of alkaline earth metal ions and the ammonium cation (ΔE_{pa} : 21 mV for Ca²⁺, 27 mV for Sr²⁺, 54 mV for Ba²⁺, 21 mV for NH₄⁺). This is likely due to a generally enhanced affinity of this host for cations because of its greater number of donor atoms and, in the former case, the larger charge density of alkaline earth metal cations in comparison to the alkali metal cations. The response of **3** to alkaline earth metal cations but not alkali metal cations is notable and suggests potential application in the selective sensing of the former. Crownophane **3** shows the greatest electrochemical response to Ba²⁺ with its first oxidation potential anodically shifted 54 mV from that of the free ligand (Fig. 4). Similar to **3**, a TTF-containing crownophane of comparable size displays a preference for alkaline earth versus alkali metal cations.^{8a} In this case, the TTF host showed a 100 mV anodic shift in its first oxidation potential in the presence of a stoichiometric amount of Ba²⁺. Interestingly, however, an X-ray structure of the TTF-crownophane complex with Ba²⁺ shows only the participation of the polyether subunit in coordination of the metal cation.^{8a} Perhaps, then, it is not surprising that compound **3** is the only Wurster's crownophane to

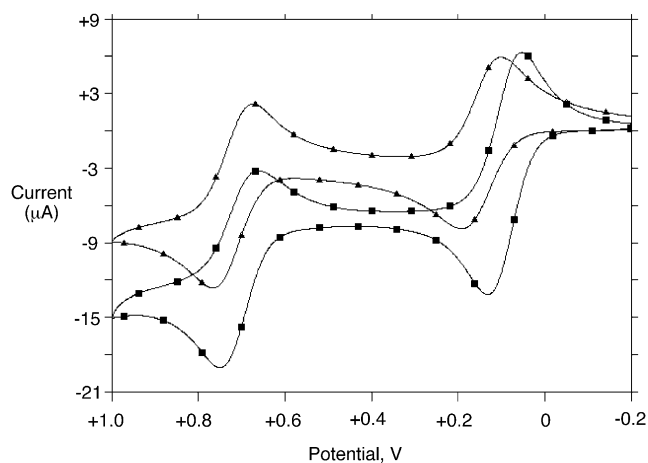


Figure 4. Cyclic voltammograms (0.1 M TEABF₄, CH₃CN, 100 mV/s) of Wurster's crownophane **3** (■), and **3** in the presence of 1.2 equiv of Ba(OTf)₂ (▲).

demonstrate an ability to form complexes with hard cations among the three ligands studied. In complexes of **3**, the second oxidation potential is unshifted relative to that of the free crownophane (see Fig. 4, for example) indicating that the second oxidation in the cyclic voltammogram of each complex is, in actuality, that of the free ligand. Therefore, the dicationic form of **3** does not support complexation with ejection of the ion from the macrocyclic cavity presumed upon its formation.

2.4. Computational analysis

Proton NMR spectra of **1**, **2** and **3** show a single aromatic peak indicative of the equilibration of *cis* and *trans* conformers in solution. Consistent with these results, gas-phase B3LYP/6-31 + G* calculations reveal that the *cis* and *trans* conformers of **1** are very close in energy, with the latter only 0.59 kcal/mol more stable than the former. An analysis of each of these conformers supports the electrochemical results that Wurster's crownophanes should indeed oxidize more easily than TMPD (Fig. 5) through the intramolecular stabilization of the radical cationic form of the phenylenediamine moiety by the polyether subunit. In the neutral state, the dipole moment of each conformer is oriented with the negative end directed toward the electron-rich phenylenediamine moiety. Upon oxidation, the positive charge of the radical cation is localized on the phenylenediamine portion of the Wurster's crownophane. The calculated natural atomic charges, listed in Figure 5, become considerably less negative, or more positive, on the phenylenediamine heavy atoms (excluding the terminal methyl groups) thereby corroborating this view. Not only does the magnitude of the dipole moment significantly decrease (2.532–1.131 D for the *trans*, 4.209 to 2.996 D for the *cis*), but the direction of the dipole moment changes as well, with the positive end residing near the phenylenediamine group. Motivated by the ensuing stabilization of the radical cation charge, the molecular geometry responds to this shift in the charge distribution by decreasing the distance between the

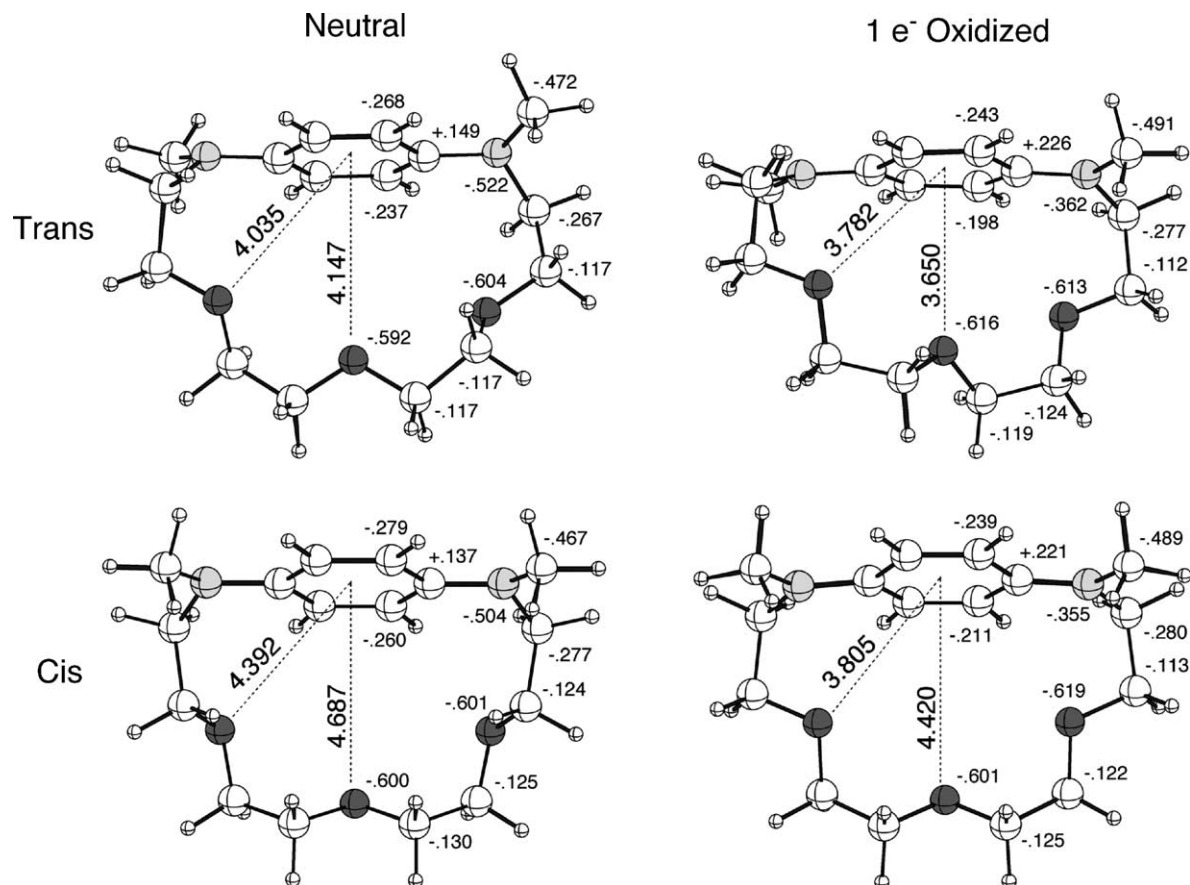


Figure 5. B3LYP/6-31 + G* and UB3LYP/6-31-G* optimized geometries of the neutral and radical cation states, respectively, of the *cis* and *trans* forms of compound **1**. Natural atomic charges are listed beside the symmetry unique heavy atoms.

oxygen donor groups of the crown ether and the phenylenediamine moiety. Figure 5 illustrates how, upon oxidation, the average X–O_{ave} distance (where X is the centroid of the phenyl ring) in the trans isomer decreases by 0.334 Å, while X–O_{ave} in the cis conformer decreases by 0.480 Å. It is interesting to note that in the C₂-symmetric trans conformer, the distal X–O distance decreases more than the proximal X–O distance (0.497 Å vs 0.253 Å), while for the C_s-symmetric cis conformer, the proximal X–O distance decreases more than the distal X–O distance (0.587 Å vs 0.267 Å). That the cis conformer exhibits both the largest ΔX–O_{ave} as well as the largest discrete ΔX–O helps explain the lower calculated ionization potential for it relative to that for trans (124.7 vs 128.3 kcal/mol, respectively).

3. Conclusion

We have established a simple synthetic procedure to the Wurster's crownphanes and demonstrated, both electrochemically and computationally, a relationship between their structure and ease of oxidation. The general lack of response to alkali metal cations and the modest magnitude of the electrochemical shifts of **3** in the presence of cations indicates that the electron-rich π face is a poor ligating group for hard cations in polar media. As such, in contrast to the Wurster's crown ethers, complexes of the Wurster's crownphanes presumably involve little contribution from the redox center. However, the anodic shift in the first oxidation potential of **3** in response to alkaline earth but not alkali metal cations is notable and demonstrates a selectivity among the hard cations that is not observed in the alternate Wurster's crown ether topology.

4. Experimental

4.1. General information

All solvents and reagents were of reagent grade quality, purchased commercially, and unless noted, used without further purification. All reactions were carried out under dry argon unless stated otherwise. The precursor *N,N'*-dimethyl-*p*-phenylenediamine dihydrobromide was synthesized in three steps from 1,4-phenylenediamine using a modification of the procedure of Michaelis, et al.¹² As full experimental details and characterization were not included in that report, we provide procedures and characterization in this work. All ¹H and ¹³C NMR spectra were recorded on a JEOL Eclipse 270 MHz NMR spectrometer in chloroform-*d*, acetone-*d*₆ or deuterium oxide (Aldrich Chemical Co.) referencing peaks to solvent. Mass spectra were acquired by the analytical services laboratories at Northwestern University and the University of Texas at Austin. Preparative chromatography columns were packed with activated neutral aluminum oxide (~150 mesh, 58 Å surface area). Alumina (60 GF₂₅₄ Neutral Type E) was used for radial chromatography (Chromatotron, Harrison Research, Model 7924 T).

4.1.1. Synthesis of *N,N'*-di-*p*-toluenesulfonyl-1,4-phenylenediamine. A solution of NaOH (2 M, 200 mL) and 1,4-phenylenediamine (10.0 g, 92.5 mmol) was cooled to 0 °C.

A solution of *p*-toluenesulfonyl chloride (38.6 g, 202 mmol) in diethyl ether (200 mL) was added dropwise. The dark reddish brown solution was allowed to warm to room temperature overnight. The reaction mixture, containing a large amount of product as precipitate, was then neutralized with the careful addition of 1 M hydrochloric acid to complete the precipitation process. The precipitate was collected and washed with water. The crude product was washed with boiling methanol, filtered and then washed with ethyl ether to afford the desired product (38.6 g, 90%) as a tan powder. ¹H NMR (CD₃COCD₃): δ 2.38 (s, 6H, ArCH₃), 7.05 (s, 4H, Ar), 7.32 (d, *J*=8.0 Hz, 4H, Ar), 7.63 (d, *J*=8.0 Hz, 4H, Ar), 8.79 (s, 2H, NH). ¹³C NMR (CD₃COCD₃): δ 21.8, 123.3, 128.3, 130.7, 135.9, 144.7. MS (EI): *m/z* (%) 416 (100) [M⁺]. HR CI MS *m/z* 417.0937 [M+H⁺] (calcd for C₂₀H₂₁N₂O₄S₂, *m/z* 417.0943).

4.1.2. Synthesis of *N,N'*-dimethyl-*N,N'*-di-*p*-toluenesulfonyl-1,4-phenylenediamine. To a 60% dispersion of NaH in mineral oil (2.2 g) and *N,N'*-di-*p*-toluenesulfonyl-1,4-phenylenediamine (10.0 g, 24.0 mmol) was added anhydrous DMF (100 mL). The reaction mixture was then heated at 90 °C for 60 min. Upon cooling to room temperature, a solution of methyl iodide (3.15 mL, 51.0 mmol) in DMF (100 mL) was added dropwise and the reaction stirred for 12 h. The solvent was removed in vacuo and the resulting solids washed thoroughly with water. The crude reaction product was washed with hot methanol and then ether to afford the desired product as an off-white powder (9.66 g, 90%). ¹H NMR (CDCl₃): δ 2.41 (s, 6H, ArCH₃), 3.13 (s, 6H, NCH₃), 7.00 (s, 4H, Ar), 7.22 (d, *J*=8.2 Hz, 4H, Ar), 7.40 (d, *J*=8.2 Hz, 4H, Ar). ¹³C NMR (CDCl₃): δ 22.1, 38.4, 127.2, 128.3, 129.9, 133.7, 140.8, 144.3. MS (FAB): *m/z* 445.1 [M+H⁺], 467.1 [M⁺+Na⁺]. HR CI MS *m/z* 445.1253 [M+H⁺] (calcd for C₂₂H₂₅N₂O₄S₂, *m/z* 445.1256).

4.1.3. Synthesis of *N,N'*-dimethyl-*p*-phenylenediamine dihydrobromide. Treatment of *N,N'*-dimethyl-*N,N'*-di-*p*-toluenesulfonyl-1,4-phenylenediamine (15 g, 33.8 mmol) with HBr in acetic acid (30 wt%, 225 mL) in the presence of phenol (26 g, 276 mmol) at 90 °C for 40 h afforded a tan precipitate. The precipitate was isolated by filtration and washed with ether to yield a white solid (7.91 g, 79%). ¹H NMR (D₂O): δ 2.76 (s, 6H, NCH₃), 6.57 (s, 4H, Ar). ¹³C NMR (D₂O): δ 39.6, 126.9, 140.2. HR EI MS *m/z* 136.0998 [M⁺] (calcd for C₈H₁₂N₂, *m/z* 136.1000).

4.1.4. Syntheses of crownphanes 1–6. The three congeners **1**, **2** and **3** were synthesized according to the same procedure with **4**, **5** and **6** being isolated, respectively, from the same reaction mixtures. Tetraethylene, pentaethylene and hexaethylene glycol ditosylate were used to synthesize **1**, **2** and **3**, respectively. The following representative procedure is for the synthesis of **1**. *N,N'*-dimethyl-*p*-phenylenediamine dihydrobromide (1.00 g, 3.36 mmol) and cesium carbonate (4.88 g, 15.0 mmol) were added to dry acetonitrile (350 mL). Following the addition of tetraethylene glycol ditosylate (2.10 g, 4.20 mmol), the reaction was stirred at reflux for 72 h. The solvent was then removed in vacuo. The resulting solid was partitioned between water and CHCl₃. The organic layer was dried with magnesium sulfate and filtered. The crude product mixture

was purified via column chromatography (alumina, CHCl_3 as eluent) followed by radial chromatography (alumina, CHCl_3 as eluent). The corresponding larger ring, '2+2' cycloaddition product **4**, was isolated in 5% yield as a slower moving fraction (in comparison to **1**). Mixtures containing **1** and **4** could be separated by crystallization from methanol with **4** forming colorless crystals and **1** remaining in solution. In the cases of the other pairs of crownphanes (**2** and **5**, **3** and **6**), chromatography was the only purification method used. With the exception of **4**, all crownphanes were isolated as light brown oils. Yield of **1**: 0.216 g (23%). Compound **1**: ^1H NMR (CDCl_3): δ 2.84 (s, 6H, NCH_3), 3.17 (t, $J=5.2$ Hz, 4H, CH_2N), 3.30 (t, $J=4.9$ Hz, 4H, CH_2O), 3.50 (t, $J=4.6$ Hz, 4H, CH_2O), 3.60 (t, $J=4.7$ Hz, 4H, CH_2O), 6.81 (s, 4H, Ar). ^{13}C NMR (CDCl_3): δ 38.4, 53.6, 68.0, 69.8, 70.6, 116.6, 143.1. MS (EI): m/z (%) 294 (100) [M^+], 295 (17.5) [$\text{M}+1^+$]. HR MS (ESI, 70 eV) m/z 294.19390 [M^+] (calcd for $\text{C}_{16}\text{H}_{26}\text{N}_2\text{O}_3$, m/z 294.19434). Compound **2** Yield 25%. ^1H NMR (CDCl_3): δ 2.86 (s, 6H, NCH_3), 3.42 (m, 8H, CH_2N , CH_2O), 3.53 (br m, 8H, CH_2O), 3.63 (t, $J=5.0$ Hz, 4H, CH_2O), 6.80 (s, 4H, Ar). ^{13}C NMR (CDCl_3): δ 39.2, 53.7, 68.6, 70.6, 70.8, 115.1, 141.8. MS (EI): m/z (%) 337.1 (100) [$\text{M}-1^+$], 338.1 (17.5) [M^+]. HR MS (ESI, 70 eV) m/z 338.22111 [M^+] (calcd for $\text{C}_{18}\text{H}_{30}\text{N}_2\text{O}_4$, m/z 338.22056). Compound **3**: Yield 21%. ^1H NMR (CDCl_3): δ 2.87 (s, 6H, NCH_3), 3.41 (t, $J=5.6$ Hz, 4H, CH_2N), 3.60 (m, 20H, CH_2O), 6.80 (s, 4H, Ar). ^{13}C NMR (CDCl_3): δ 39.5, 54.7, 68.8, 70.7, 70.9, 115.3, 142.5. MS (EI): m/z (%) 382 (100) [M^+], 383 (29.5) [$\text{M}+1^+$]. HR MS (ESI, 70 eV) m/z 382.24693 [M^+] (calcd for $\text{C}_{20}\text{H}_{34}\text{N}_2\text{O}_5$, m/z 382.24677). Compound **4**: mp (uncorrected): 66–67 °C. ^1H NMR (CDCl_3): δ 2.85 (s, 12H, CH_3N), 3.36 (m, 8H, CH_2N), 3.59 (m, 24H, CH_2O), 6.71 (s, 8H, Ar). ^{13}C NMR (CDCl_3): δ 39.4, 53.6, 68.5, 70.5, 114.8, 142.0. MS (ESI): m/z (%) 588.38 (100) [M^+], 589.39 (37.5) [$\text{M}+1^+$], 590.39 (8.1) [$\text{M}+2^+$]. HR MS (ESI, 70 eV) m/z 588.39053 [M^+] (calcd for $\text{C}_{32}\text{H}_{52}\text{N}_4\text{O}_6$, m/z 588.38867). Compound **5**: Yield 3%. ^1H NMR (CDCl_3): δ 2.85 (s, 12H, CH_3N), 3.39 (m, 8H, CH_2N), 3.61 (m, 32H, CH_2O), 6.68 (s, 8H, Ar). ^{13}C NMR (CDCl_3): δ 39.6, 53.8, 68.7, 70.6, 115.1, 142.2. MS (EI): m/z (%) 676 (100) [M^+], 677 (41) [$\text{M}+1^+$]. HR MS (ESI, 70 eV) m/z 676.44241 [M^+] (calcd for $\text{C}_{36}\text{H}_{60}\text{N}_4\text{O}_8$, m/z 676.44110). Compound **6**: Yield 3%. ^1H NMR (CDCl_3): δ 2.87 (s, 12H, CH_3N), 3.40 (br, 8H, CH_2N), 3.61 (m, 40H, CH_2O), 6.73 (s, 8H, Ar). ^{13}C NMR (CDCl_3): δ 39.8, 53.8, 68.6, 70.6, 115.1, 142.2. MS (EI): m/z (%) 764.3 (100) [M^+], 765.3 (59) [$\text{M}+1^+$]. HR MS (ESI, 70 eV) m/z 764.4931 (calcd for $\text{C}_{40}\text{H}_{68}\text{O}_{10}\text{N}_4$, m/z 764.4930).

4.2. Computational methods

Full-gradient geometry optimizations¹³ were performed in redundant internal coordinates¹⁴ with ab initio DFT methods. Becke's three-parameter hybrid exchange functional (B3)¹⁵ was used in conjunction with the Lee–Yang–Parr correlation functional (LYP)¹⁶ and a 6-31+G* basis.¹⁷ Previous studies have demonstrated that a careful application of theory is required to accurately model the hybridization of the amine groups and their orientation with respect to the plane of the phenyl ring in the electron rich phenylenediamine moiety.^{18,19} In this context, the B3LYP/6-31+G* and UB3LYP/6-31+G* methods should be

reliable for the evaluation of the neutral and radical cation forms of the Wurster's crownphanes, respectively. Atomic charges were calculated by the natural population analysis (NPA)/natural bond orbital (NBO) method.²⁰ All calculations were performed with either the G94²¹ or G98²² program suite.

4.3. Cyclic voltammetry

Tetraethylammonium tetrafluoroborate (TEABF_4) was purchased as electrochemical grade from Acros and was not purified further. Acetonitrile (low water 99.9+% grade, Burdick and Jackson) was distilled from CaH_2 . Electrochemical experiments were performed using a BAS CV-50W Voltammetric Analyzer (Bioanalytical Systems, Inc.). The electrochemical system was comprised of a platinum working electrode, a Ag/AgCl reference electrode and a platinum wire auxiliary electrode. Acetonitrile solutions (containing 0.1 M TEABF_4 electrolyte and 1.0–1.5 mM ligand) were placed in an electrochemical cell and purged with dry N_2 . For cation binding experiments, 1.2 equiv of salt were used. The salts used were LiBF_4 , $\text{NaClO}_4 \cdot \text{H}_2\text{O}$, KPF_6 , RbClO_4 , CsClO_4 , $\text{Mg}(\text{ClO}_4)_2$, $\text{Ca}(\text{ClO}_4)_2$, $\text{Sr}(\text{ClO}_4)_2$, $\text{Ba}(\text{OTf})_2$, and NH_4PF_6 . Rubidium, cesium, and all alkaline earth salts were stirred for 1 h prior to obtaining a voltammogram; all others were stirred 5 min or until no further change in oxidation potential was observed.

4.4. X-ray experimental for **4**

Crystals were grown from a methanolic solution of **4**. The data crystal was cut from a larger crystal and had approximate dimensions of $0.31 \times 0.31 \times 0.25$ mm. The data were collected on a Nonius Kappa CCD diffractometer using a graphite monochromator with Mo $\text{K}\alpha$ radiation ($\lambda = 0.71073$ Å). A total of 538 frames of data were collected using ω -scans with a scan range of 1° and a counting time of 27 s per frame. The data were collected at 153 K using an Oxford Cryostream low temperature device. Details of crystal data, data collection and structure refinement are listed in Table 2. Data reduction were performed using DENZO-SMN.²³ The structure was solved by direct methods using SIR97²⁴ and refined by full-matrix least-squares on F^2 with anisotropic displacement parameters for the non-H atoms using SHELXL-97.²⁵ The hydrogen atoms on carbon were calculated in ideal positions with isotropic displacement parameters set to $1.2 \times \text{Ueq}$ of the attached atom ($1.5 \times \text{Ueq}$ for methyl hydrogen atoms).

There are two crystallographically independent molecules per asymmetric unit. Each molecule lies around a different crystallographic inversion center. Molecule 1, composed of non-H atoms labeled O1 to C21, resides around an inversion center at 0, 1, 1/2. Molecule 2, composed of non-H atoms labeled O22–C42, resides around an inversion center at 1, 1, 0. The function, $\sum w(|F_o|^2 - |F_c|^2)^2$, was minimized, where $w = 1/[(\sigma(F_o))^2 + (0.0787 \times P)^2 + (0.9425 \times P)]$ and $P = (|F_o|^2 + 2|F_c|^2)/3$. $R_w(F^2)$ was refined to 0.177, with $R(F)$ equal to 0.0587 and a goodness of fit, $S = 1.01$. Definitions used for calculating $R(F)$, $R_w(F^2)$ and S are given below.²⁶ The data were corrected for secondary extinction effects. The correction takes the form: $F_{\text{corr}} = kF_o/[1 + (7(2) \times 10^{-6}) \times F_c^2 \lambda^3 / (\sin 2\theta)]^{0.25}$ where k is the overall scale factor. Neutral

Table 2. Crystallographic data for compound 4

Empirical formula	C ₃₂ H ₅₂ N ₄ O ₆
Formula weight	588.78
Temperature	153(2) K
Wavelength	0.71073 Å
Crystal system	Triclinic
Space group	<i>P</i> −1
Unit cell dimensions	<i>a</i> = 9.7927(1) Å, <i>α</i> = 69.800(1)° <i>b</i> = 11.5821(2) Å, <i>β</i> = 74.668(1)° <i>c</i> = 16.1542(2) Å, <i>γ</i> = 69.689(1)°
Volume	1590.70(4) Å ³
Z	2
Density (calculated)	1.229 mg/m ³
Absorption coefficient	0.085 mm ^{−1}
<i>F</i> (000)	640
Crystal size	0.35 × 0.31 × 0.25 mm ³
Theta range for data collection	2.97–27.49°
Index ranges	−9 ≤ <i>h</i> ≤ 12, −12 ≤ <i>k</i> ≤ 15, −19 ≤ <i>l</i> ≤ 20
Reflections collected	11,329
Independent reflections	7279 [<i>R</i> (int) = 0.0246]
Completeness to theta = 27.49°	99.7%
Absorption correction	None
Refinement method	Full-matrix least-squares on <i>F</i> ²
Data/restraints/parameters	7279/0/380
Goodness-of-fit on <i>F</i> ²	1.012
Final <i>R</i> indices [<i>I</i> > 2σ(<i>I</i>)]	<i>R</i> 1 = 0.0587, <i>wR</i> 2 = 0.1503
<i>R</i> indices (all data)	<i>R</i> 1 = 0.1135, <i>wR</i> 2 = 0.1773
Extinction coefficient	7.2(17) × 10 ^{−6}
Largest diff. peak and hole	0.538 and −0.460 e Å ^{−3}

atom scattering factors and values used to calculate the linear absorption coefficient are from the International Tables for X-ray Crystallography (1992).²⁷ All figures were generated using SHELXTL/PC.²⁸ Crystallographic data (excluding structure factors) for the structure in this paper have been deposited with the Cambridge Crystallographic Data Centre as supplementary publication number CCDC 274269. Copies of the data can be obtained, free of charge, on application to CCDC, 12 Union Road, Cambridge CB2 1EZ, UK [fax: +44 1233 336033 or e-mail: deposit@ccdc.cam.ac.uk].

Acknowledgements

This work was supported by the Robert A. Welch Foundation (AT-1527).

References and notes

- (a) Beer, P. D.; Gale, P. A.; Chen, G. Z. *Coord. Chem. Rev.* **1999**, *185–186*, 3–36. (b) Kaifer, A. E.; Mendoza, S. In Gokel, G. W., Atwood, J. L., Davies, J. E., MacNicol, D. D., Vögtle, F., Eds.; *Comprehensive Supramolecular Chemistry*; Pergamon: Oxford, 1996; Vol. 1, pp 701–732. (c) Boulas, P. L.; Gomez-Kaifer, M.; Echegoyen, L. *Angew. Chem., Int. Ed.* **1998**, *37*, 216–247. (d) Allgeier, A. M.; Mirkin, C. A. *Angew. Chem., Int. Ed.* **1998**, *37*, 894–908. (e) Saji, T.; Kinoshita, I. *J. Chem. Soc., Chem. Commun.* **1986**, 716–717.
- (a) Sibert, J. W.; Forshee, P. B. *Inorg. Chem.* **2002**, *41*, 5928–5930. (b) Sibert, J. W.; Seyer, D. J.; Hundt, G. R. *J. Supramol. Chem.* **2002**, *2*, 335–342. (c) Sibert, J. W. U.S. Patent 6,262,258, 2001. (d) Sibert, J. W. U.S. Patent 6,441,164, 2002.
- (a) Pearson, A. J.; Hwang, J. T. *Tetrahedron Lett.* **2001**, *42*, 3533–3536. (b) Pearson, A. J.; Hwang, J. T.; Ignatov, M. E. *Tetrahedron Lett.* **2001**, *42*, 3537–3540. (c) Pearson, A. J.; Hwang, J. T. *Tetrahedron Lett.* **2001**, *42*, 3541–3543. (d) Zhang, X.; Buchwald, S. L. *J. Org. Chem.* **2000**, *65*, 8027–8031. (e) Liu, X.; Eisenberg, A. H.; Stern, C. L.; Mirkin, C. A. *Inorg. Chem.* **2001**, *40*, 2940–2941. (f) Crochet, P.; Malval, J. P.; Lapouyade, R. *Chem. Commun.* **2000**, 289–290.
- Wurster, C. *Ber. Dtsch. Chem. Ges.* **1879**, *12*, 522–528.
- For a review of crownphanes, see Inokuma, S.; Sakai, S.; Nishimura, J. *Top. Curr. Chem.* **1994**, *174*, 87–118.
- (a) Dougherty, D. A. *Science* **1996**, *271*, 163–168. (b) Hu, J.; Barbour, L.; Gokel, G. W. *J. Am. Chem. Soc.* **2002**, *124*, 10940–10941.
- Timko, J. M.; Moore, S. S.; Walba, D. M.; Hiberty, P. C.; Cram, D. J. *J. Am. Chem. Soc.* **1977**, *99*(13), 4207–4219.
- See, for example (a) Le Derf, F.; Mazari, M.; Mercier, N.; Levillain, E.; Richomme, P.; Becher, J.; Garín, J.; Orduna, J.; Gorgues, A.; Sallé, M. *Inorg. Chem.* **1999**, *38*, 6096–6100. (b) Le Derf, F.; Mazari, M.; Mercier, N.; Levillain, E.; Richomme, P.; Becher, J.; Garín, J.; Orduna, J.; Gorgues, A.; Sallé, M. *Chem. Commun.* **1999**, 1417–1418.
- Staab, J. A.; Gabel, G.; Krieger, C. *Chem. Ber.* **1987**, *120*, 269–273.
- Takemura, H.; Takehara, K.; Ata, M. *Eur. J. Org. Chem.* **2004**, 4936–4941.
- Mortimer, R. J.; Weightman, J. S. *J. Electroanal. Chem.* **1996**, *418*, 1–7.
- Michaelis, L.; Schubert, M. P.; Granick, S. *J. Am. Chem. Soc.* **1939**, *61*, 1981–1992.
- Pulay, P. *Mol. Phys.* **1969**, *17*, 197–204.
- Peng, C.; Ayala, P. Y.; Schlegel, H. B.; Frisch, M. J. *J. Comput. Chem.* **1996**, *17*, 49–56.
- Becke, A. D. *J. Chem. Phys.* **1993**, *98*, 5648–5652.
- Lee, C.; Yang, W.; Parr, R. G. *Phys. Rev. B* **1988**, *37*, 785–789.
- Ditchfield, R.; Hehre, W. J.; Pople, J. A. *J. Chem. Phys.* **1971**, *54*, 724–728. Hehre, W. J.; Ditchfield, R.; Pople, J. A. *J. Chem. Phys.* **1972**, *56*, 2257–2261. Clark, T.; Chandrasekhar, J.; Spitznagel, G. W.; Schleyer, P. v. R. *J. Comp. Chem.* **1983**, *4*, 294–301. Frisch, M. J.; Pople, J. A.; Binkley, J. S. *J. Chem. Phys.* **1984**, *80*, 3265–3269.
- (a) Brouwer, A. M.; Wilbrandt, R. *J. Phys. Chem.* **1996**, *100*, 9678–9688. (b) Brouwer, A. M. *J. Phys. Chem. A* **1997**, *101*, 3626–3633.
- Sponer, J.; Hobza, P. *Int. J. Quantum Chem.* **1996**, *57*, 959–970.
- Reed, A. E.; Curtiss, L. A.; Weinhold, F. *Chem. Rev.* **1988**, *88*, 899–926.
- Frisch, M. J.; Trucks, G. W.; Schlegel, H. B.; Gill, P. M. W.; Johnson, B. G.; Robb, M. A.; Cheeseman, J. R.; Keith, T. A.; Petersson, G. A.; Montgomery, J. A.; Raghavachari, K.; Al-Laham, M. A.; Zakrzewski, V. G.; Ortiz, J. V.; Foresman, J. B.; Cioslowski, J.; Stefanov, B. B.; Nanayakkara, A.; Challacombe, M.; Peng, C. Y.; Ayala, P. Y.; Chen, W.; Wong, M. W.; Andres, J. L.; Replogle, E. S.; Gomperts, R.; Martin, R. L.; Fox, D. J.; Binkley, J. S.; Defrees, D. J.; Baker, J.; Stewart, J. J. P.; Head-Gordon, M.; Gonzalez, C.; Pople, J. A., Gaussian 94, Revision D1; Gaussian: Pittsburgh, PA, 1995.
- Frisch, M. J.; Trucks, G. W.; Schlegel, H. B.; Scuseria, G. E.; Robb, M. A.; Cheeseman, J. R.; Zakrzewski, V. G.; Montgomery, J. A., Jr.; Stratmann, R. E.; Burant, J. C.

- Dapprich, S.; Millam, J. M.; Daniels, A. D.; Kudin, K. N.; Strain, M. C.; Farkas, O.; Tomasi, J.; Barone, V.; Cossi, M.; Cammi, R.; Mennucci, B.; Pomelli, C.; Adamo, C.; Clifford, S.; Ochterski, J.; Petersson, G. A.; Ayala, P. Y.; Cui, Q.; Morokuma, K.; Malick, D. K.; Rabuck, A. D.; Raghavachari, K.; Foresman, J. B.; Chioslowski, J.; Ortiz, J. V.; Baboul, A. G.; Stefanov, B. B.; Liu, G.; Liashenko, A.; Piskorz, P.; Komaromi, I.; Gomperts, R.; Martin, R. L.; Fox, D. J.; Keith, T.; Al-Laham, M. A.; Peng, C. Y.; Nanayakkara, A.; Challacombe, M.; Gill, P. M. W.; Johnson, B.; Chen, W.; Wong, M. W.; Andres, J. L.; Gonzalez, C.; Head-Gordon, M.; Replogle, E. S.; Pople, J. A., Gaussian 98, Revision A.9; Gaussian: Pittsburgh, PA, 1998.
23. DENZO-SMN, Otwinowski, Z.; Minor, W. *Methods in Enzymology*, 276: Macromolecular Crystallography, part A, 307–326, Carter, Jr., C. W.; Sweets, R. M. Eds., Academic: London, 1997.
24. SIR97; Altomare, A.; Burla, M. C.; Camalli, M.; Cascarano, G. L.; Giacovazzo, C.; Guagliardi, A.; Moliterni, A. G. G.; Polidori, G.; Spagna, R. *J. Appl. Crystallog.* **1999**, 32, 115–119.
25. Sheldrick, G. M. *SHELXL97. Program for the Refinement of Crystal Structures*. University of Gottingen: Gottingen, Germany, 1994.
26. $R_w(F^2) = \{\sum w(|F_o|^2 - |F_c|^2)^2 / \sum w(|F_o|^4)\}^{1/2}$ where w is the weight given each reflection. $R(F) = \sum(|F_o| - |F_c|) / \sum |F_o|$ for reflections with $F_o > 4(\sigma(F_o))$. $S = [\sum w(|F_o|^2 - |F_c|^2)^2 / (n - p)]^{1/2}$, where n is the number of reflections and p is the number of refined parameters.
27. *International Tables for X-ray Crystallography*, Vol. C, Tables 4, 2, 6, 8 and 6.1.1.4, Wilson, A. J. C., Ed., Kluwer Academic: Boston, 1992.
28. Sheldrick, G. M. *SHELXTL/PC* (Version 5.03), Siemens Analytical X-ray Instruments, Inc., Madison, Wisconsin, USA, 1994.